

## Supporting Information

# Capping and etching roles of copper ions for controlled synthesis of Au-PtCu trimetallic nanorods with improved photothermal and photocatalytic activity

Xiang Long,<sup>a</sup> Yang Yang,<sup>a,b</sup> Zhen-Long Dou,<sup>a</sup> Qu-Quan Wang<sup>\*c</sup> and Li Zhou<sup>\*a</sup>

a. Key Laboratory of Artificial Micro- and Nano-structures of the Ministry of Education, Hubei Nuclear Solid Physics Key

Laboratory, School of Physics and Technology, Wuhan University, Wuhan 430072, China

b. School of Science, Hubei University of Technology, Wuhan 430068, China

c. College of Science, Southern University of Science and Technology, Shenzhen 518055, China

\*Corresponding author: Qu-Quan Wang, E-mail: qqwang@sustech.edu.cn; Li Zhou, Email: zhouli@whu.edu.cn

## COMSOL calculations:

We follow Chavez's report to calculate the cross section by COMSOL.<sup>1</sup> The optical characteristics of the studied plasmonic particles were simulated using COMSOL Multiphysics 6.0 finite-element based software. The 'Wave optics' module was used to calculate the radiative field resulting from a plane wave impinging on a 3-dimensional nanoparticle. The plane wave was defined as:  $E = E_0 e^{-ikx}$  and was polarized in the z-direction. The model of AuNR was formed by combining a cylinder and two hemispheres with a final width of 20 nm and a length of 60 nm; The Au@Pt model was achieved by covering the surface of AuNR with a layer of platinum with a final width of 21 nm and a length of 62 nm; The dumbbell-like Au-Pt (Cu) was made by coating platinum (copper) balls with a radius of 16 nm at both ends of the gold rod and bringing the final length to 78 nm. Each core-shell material was created in the model and the wavelength range from 500 nm to 1000 nm was simulated. Dielectric data for Au, Cu, and Pt were taken from COMSOL's Optical Materials database (Rakic et. al<sup>2</sup>) and a region of water was defined around the particle by setting the real part of the dielectric function equal to 1.33. The width of the region of water around the particle was equal to half the wavelength of the incident plane wave and a perfectly matched layer (PML) with the same width as the water was constructed to act as an absorber of the scattered field. The calculations are discussed in the following sections.

The absorption cross section as a function of wavelength was calculated by integrating the resistive heating losses over the volume of the nanoparticles. To calculate the scattering cross section, the dot product of the normal vector pointing outwards from the particle surface area and the scattered intensity vector was integrated across the entire particle surface for each wavelength. The extinction was determined by summing the absorption and scattering cross sections.

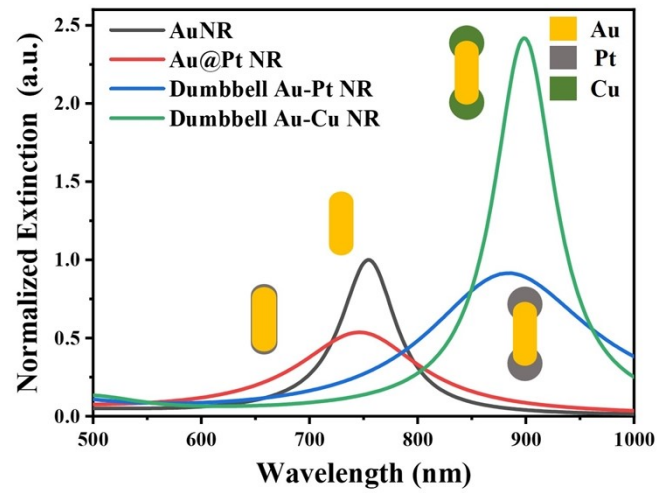


**Fig. S1** Calculated normalized extinction cross section of AuNR (black curve), Au@Pt NR (red curve), dumbbell-like Au-Pt NR (blue curve), and dumbbell-like Au-Cu NR (green curve) by COMSOL.

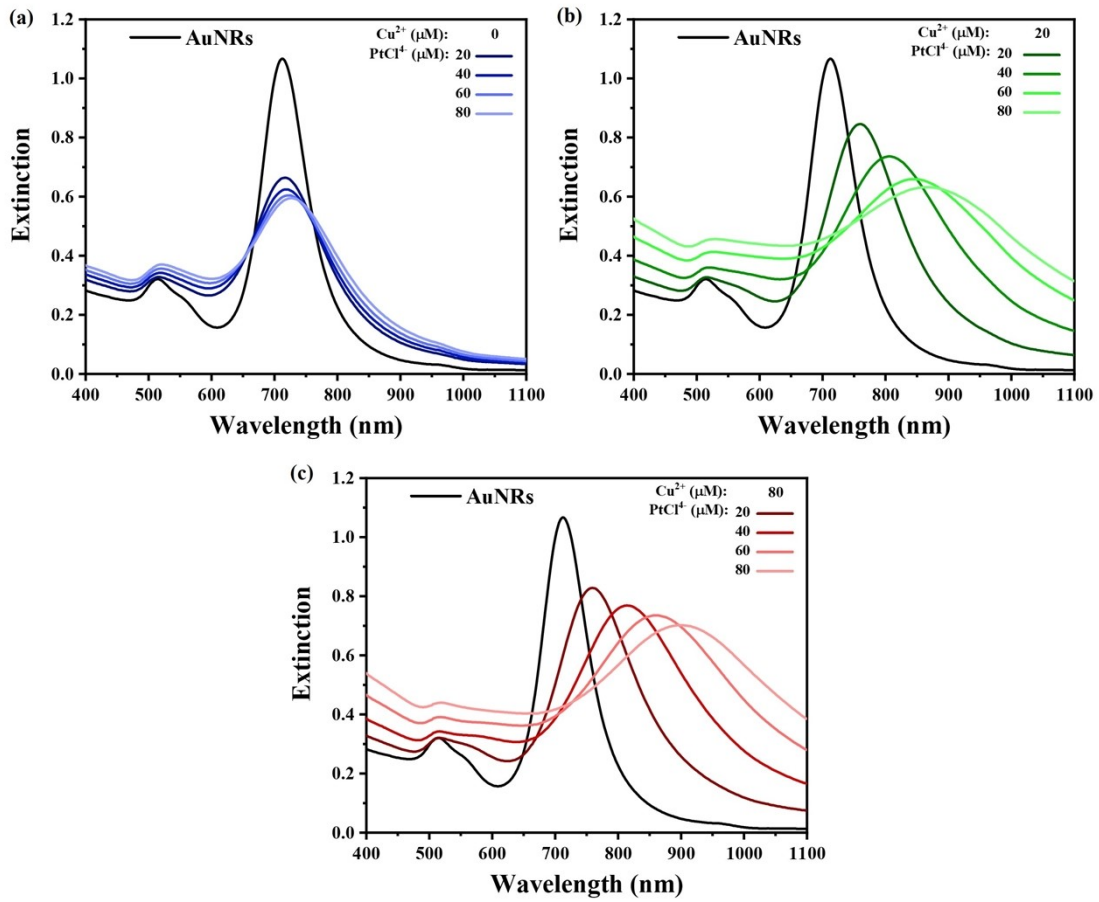


**Fig. S2** Measured extinction spectra of Au@Pt/Au-PtCu NRs with different concentrations of  $\text{CuCl}_2$  for 0  $\mu\text{M}$  (a), 20  $\mu\text{M}$  (b), and 80  $\mu\text{M}$  (c), and different concentrations of  $\text{K}_2\text{PtCl}_4$  for 20  $\mu\text{M}$ , 40  $\mu\text{M}$ , 60  $\mu\text{M}$ , and 80  $\mu\text{M}$  (from dark to bright) at 60  $^\circ\text{C}$ .

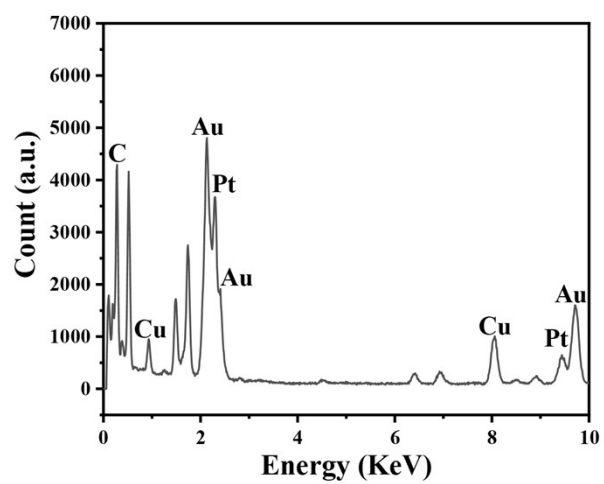


**Fig. S3** EDX spectra of dumbbell-like Au-PtCu NRs

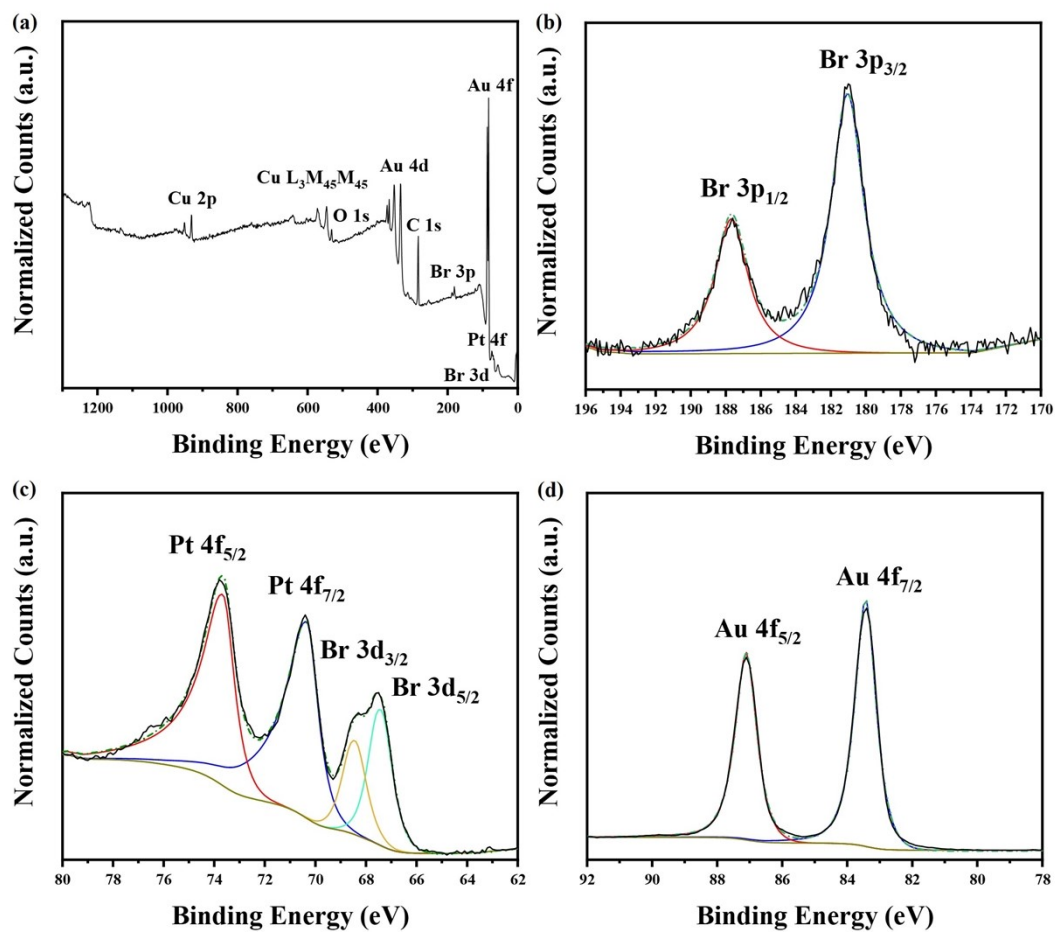


**Fig. S4** XPS spectra collected from the AuNRs in the reaction for 1 h. (a) XPS survey spectrum, (b) Br 3p, (c) Pt 4f-Br 3d and (d) Au 4f detail spectrum.

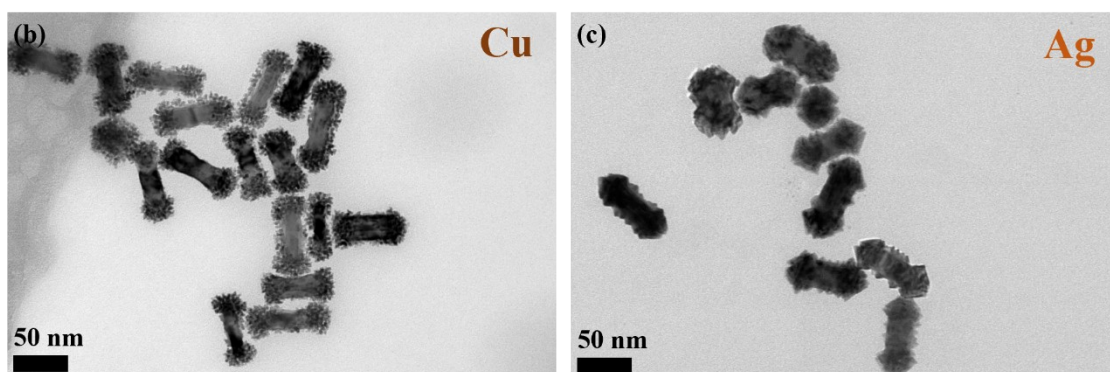
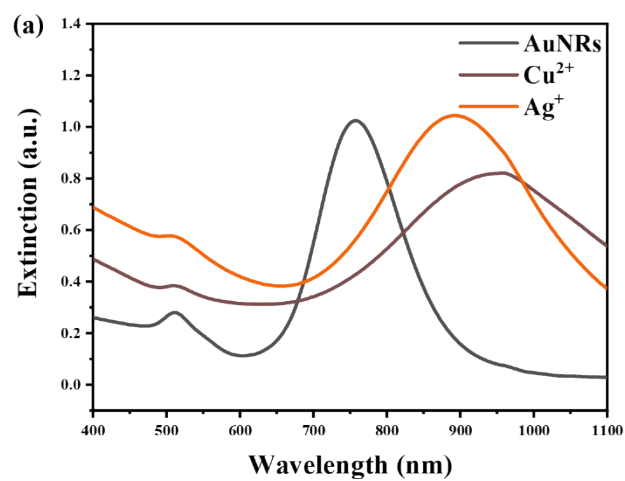


**Fig. S5** Replacing CuCl<sub>2</sub> with equal amount of AgNO<sub>3</sub> at 60 °C. (a) Extinction spectra. TEM images of (b) Cu<sup>2+</sup> experiment; (c) Ag<sup>+</sup> experiment.

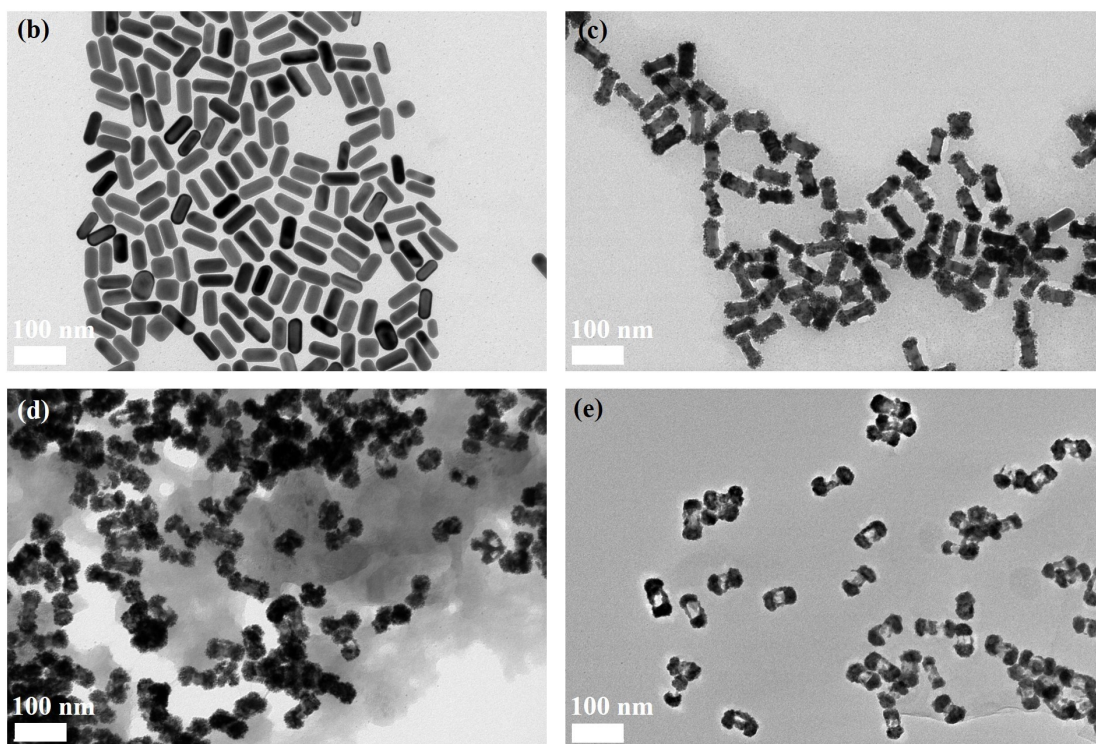
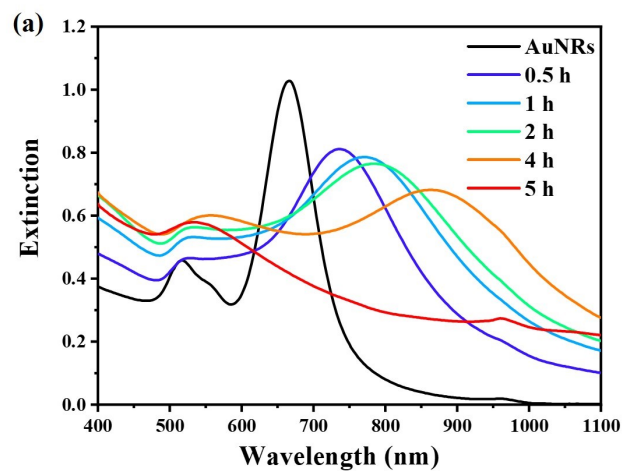


**Fig. S6** Formation process of hollow dumbbell-like Au-PtCu NRs over time. (a) Extinction spectra. TEM images at (b) 0h; (c) 0.5h; (d) 4h; (e) 5h.

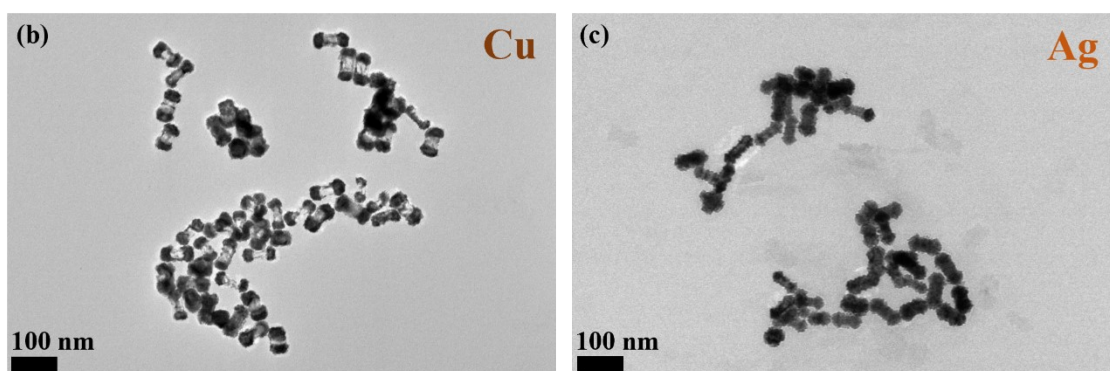
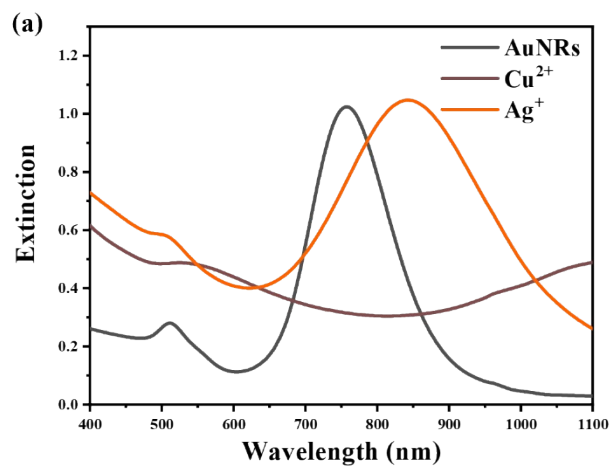


**Fig. S7** Replacing CuCl<sub>2</sub> with equal amount of AgNO<sub>3</sub> at 80 °C. (a) Extinction spectra. TEM images of (b) Cu<sup>2+</sup> experiment; (c) Ag<sup>+</sup> experiment.

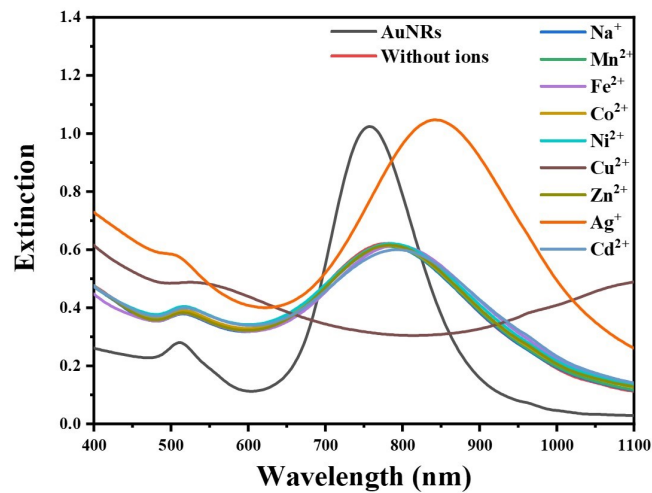


**Fig. S8** Extinction spectra of control experiment by replacing Cu<sup>2+</sup> by equal amount of Na<sup>+</sup>, Mn<sup>2+</sup>, Fe<sup>2+</sup>, Co<sup>2+</sup>, Ni<sup>2+</sup>, Zn<sup>2+</sup>, Ag<sup>+</sup>, and Cd<sup>2+</sup> at 80 °C.

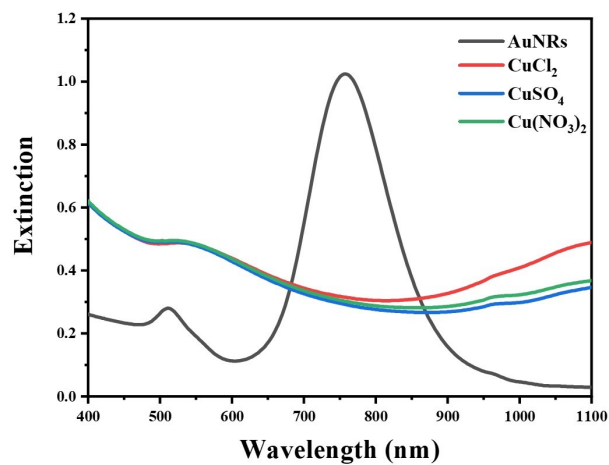


**Fig. S9** Extinction spectra of control experiment by replacing CuCl<sub>2</sub> by equal amount of CuSO<sub>4</sub>, and Cu(NO<sub>3</sub>)<sub>2</sub> at 80 °C.

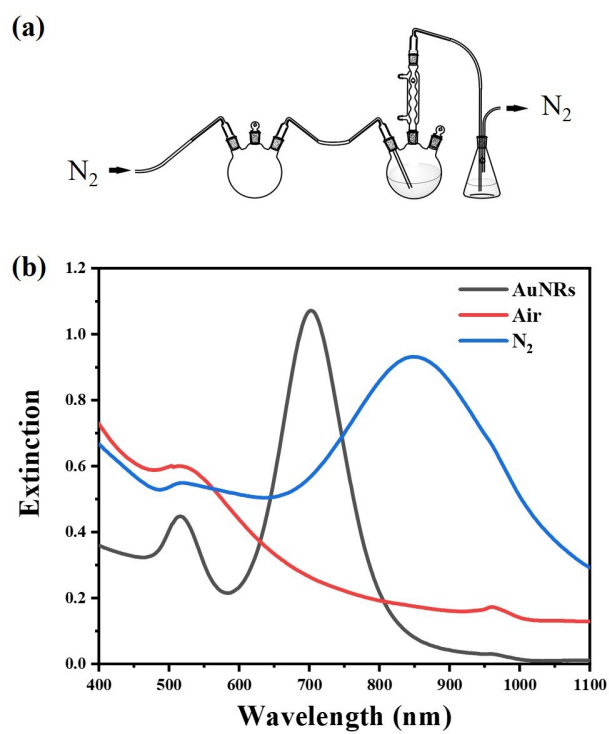


**Fig. S10** Control experiment in Air/N<sub>2</sub> environment. (a) Illustration of the experimental setup for nitrogen environment. (b) Extinction spectra.

## Calculation of photothermal conversion efficiency:

We follow Roper's report to calculate the conversion efficiency of the samples.<sup>3</sup> Due to the fact that the rate of heat transfer between two systems is proportional to the temperature difference, and that thermal radiation can be linearly approximated when the temperature difference is small, we assume that the rate of energy transfer between the solution and its surroundings is proportional to the temperature difference between them. In this experiment, a 1 mL portion of water was uniformly heated and the water further transferred heat to the quartz dish and the surrounding environment. Let  $\lambda$  denote the overall heat transfer coefficient between the water and the surrounding environment, such that the amount of heat lost by the water per unit time is  $\lambda(T - T_{suff})$ , where  $T$  is the temperature of the water and  $T_{suff}$  is the temperature of the environment.

The following differential equations can be derived for the heating and cooling processes:

Heating process:

$$(-\lambda(T - T_{surr}) + p)dt = CdT, \quad p = I_w + \eta_n I_n \#(1)$$

Cooling process:

$$-\lambda(T - T_{surr})dt = CdT \#(2)$$

Where  $C$  represents the heat capacity of water,  $t$  denotes time,  $p$  is the total heat absorbed by the solution per unit time,  $I_w$  is the heat absorption rate of water,  $I_n$  is the loss power of laser caused by nanoparticles, and  $\eta_n$  is the photothermal conversion efficiency of the nanoparticles.

The change in solution temperature over time can be obtained by solving the differential equation:

Heating process:

$$T = T_{surr} + \frac{p}{\lambda} \left(1 - e^{-\frac{\lambda t}{C}}\right) \#(3)$$

Cooling process:

$$T = T_{surr} + (T_{max} - T_{surr}) e^{-\frac{\lambda t}{C}} \#(4)$$

Where  $T_{max}$  is the equilibrium temperature.

By fitting the cooling curve (Fig. S11a, b)  $-Ln(\theta) = \frac{1}{\tau_s} t$ , the time constant for heat

conversion,  $\tau_s$ , can be obtained, where 
$$\theta = \frac{T - T_{surr}}{T_{max} - T_{surr}}$$

We can then obtain:

$$p = \lambda(T_{max} - T_{surr}) = \frac{C}{\tau_s}(T_{max} - T_{surr}) \quad \#(5)$$

$$\eta_n = \frac{p - I_w}{I_n} = \frac{\frac{C}{\tau_s}(T_{max} - T_{surr}) - I_w}{I_n} = \frac{\frac{C}{\tau_s}(T_{max} - T_{surr}) - I_w}{I_0(1 - 10^{-A})} \quad \#(6)$$

Where  $I_0$  represents the intensity of the incident laser,  $A$  denotes the extinction value of the nanoparticles at the wavelength of 808nm (Fig. S11c).

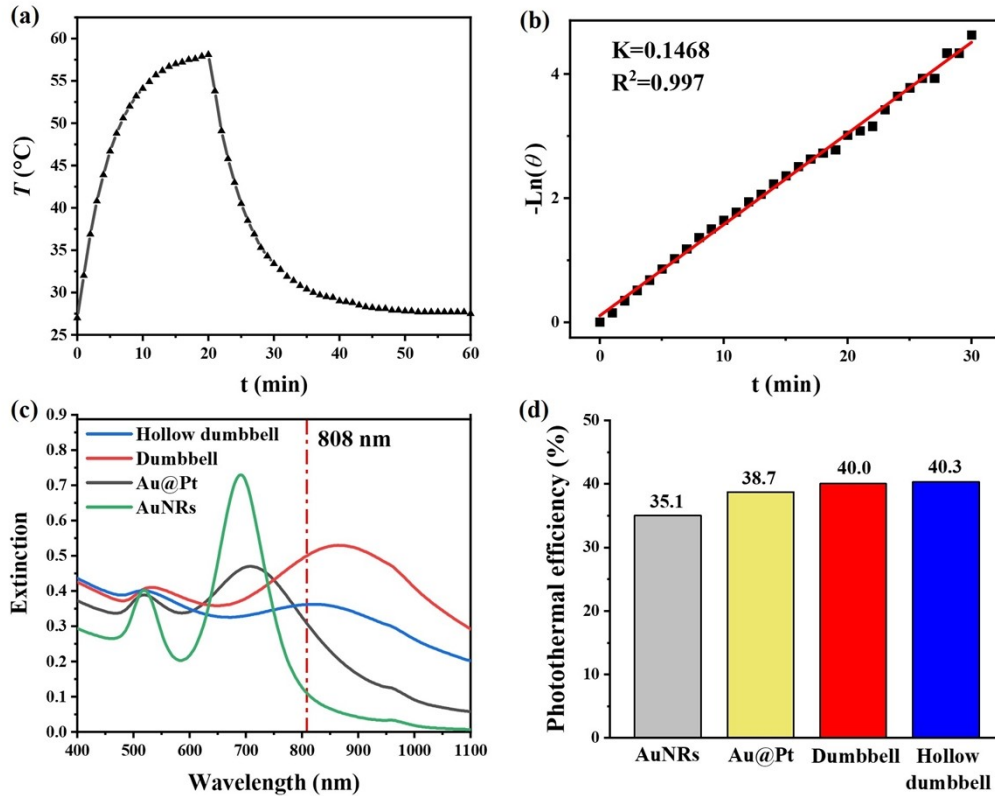


**Fig. S11** (a) Cooling process curve. (b) Fitting line between  $-\ln(\theta)$  and  $t$ . (c) Extinction spectra of the nanoparticles at the wavelength of 808nm. (d) Photothermal conversion efficiency.

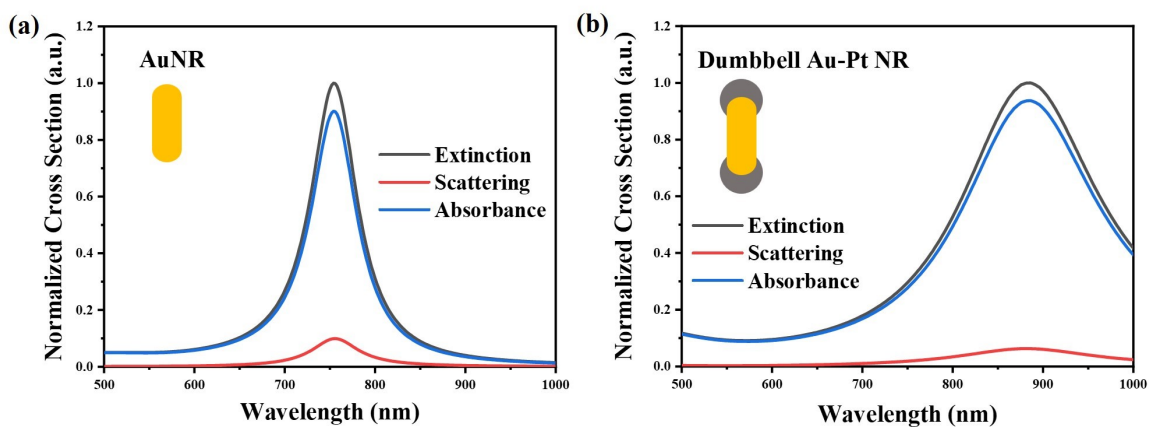


**Fig. S12** Calculated extinction (black curves), scattering (red curves), and absorbance (blue curves) cross section of AuNR (a), Au@Pt NR (b), dumbbell-like Au-Pt NR (c), and dumbbell-like Au-Cu NR (d) by COMSOL.

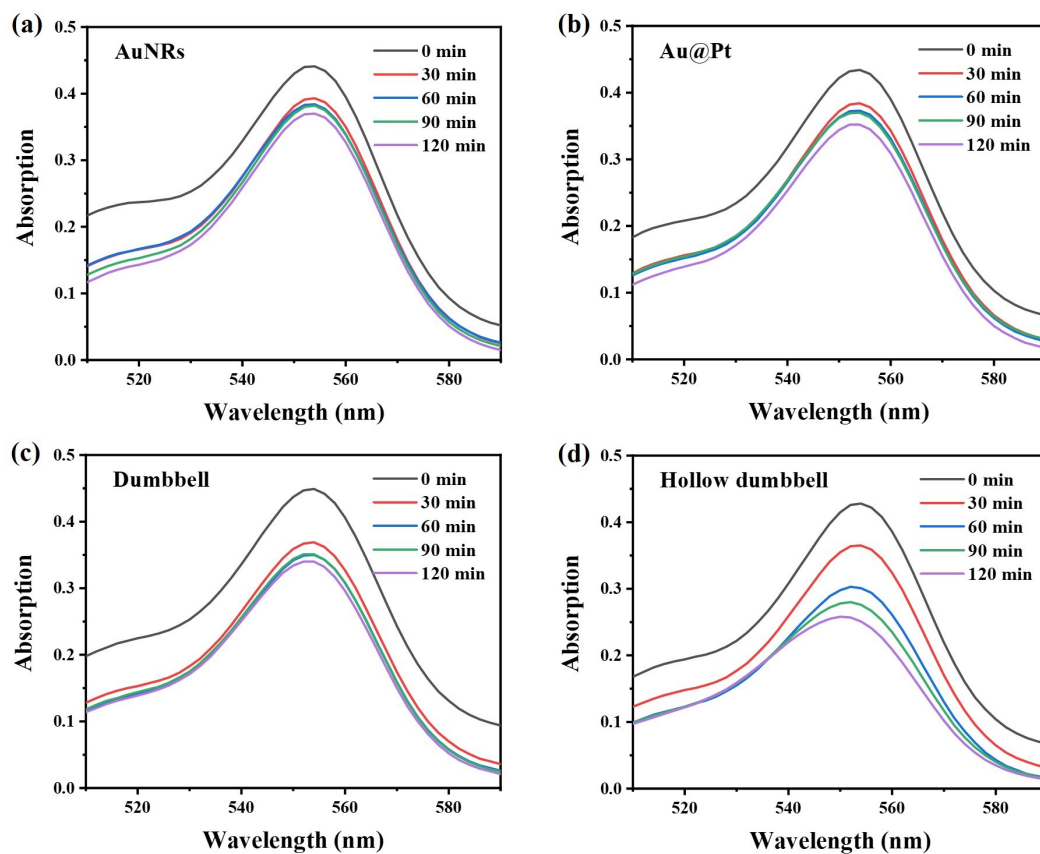


**Fig. S13** Absorption spectra of photocatalytic RhB degradation by (a) AuNRs, (b) Au-Pt NRs, (c) dumbbell-like Au-PtCu NRs, and (d) hollow dumbbell-like Au-PtCu NRs under xenon lamp irradiation.

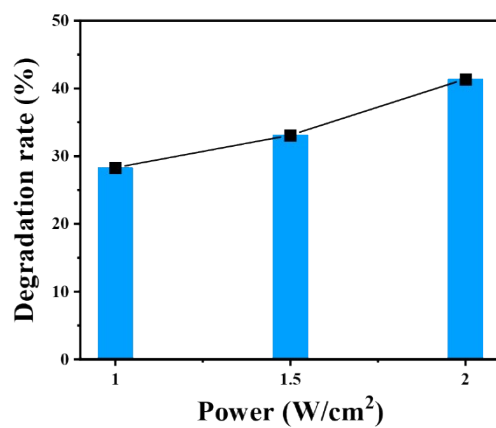


**Fig. S14** Degradation rates with different irradiation powers for the degradation of RhB using hollow dumbbell-like Au-PtCu NRs.

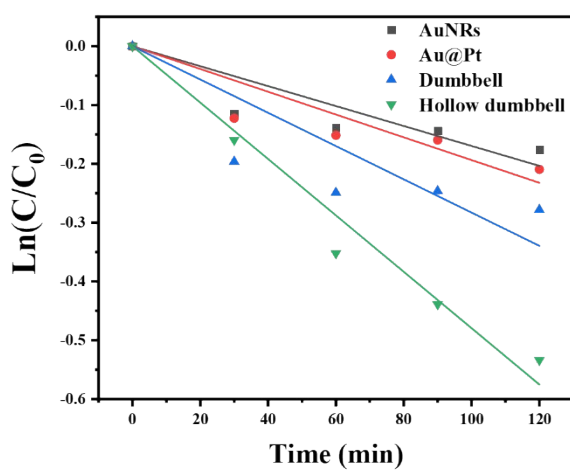


**Fig. S15** Kinetic linear fitting curves. A pseudo-first-order relationship of  $\ln(C/C_0) = -kt$  is applied to fit the experimental data, and  $k$  is reaction rate constant ( $\text{min}^{-1}$ ).

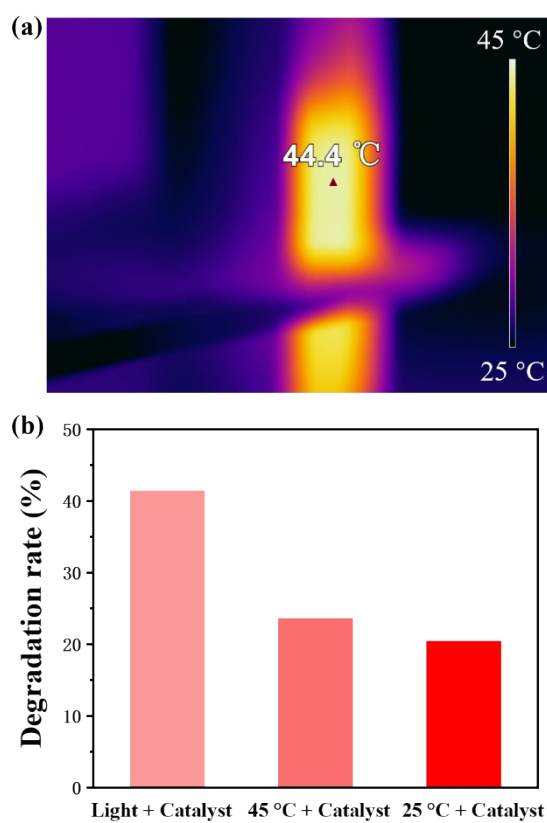


**Fig. S16** (a) Temperature measurement using infrared thermal image in the photocatalytic process of hollow dumbbell-like Au-PtCu NRs. (b) Degradation rates in the temperature-control tests.

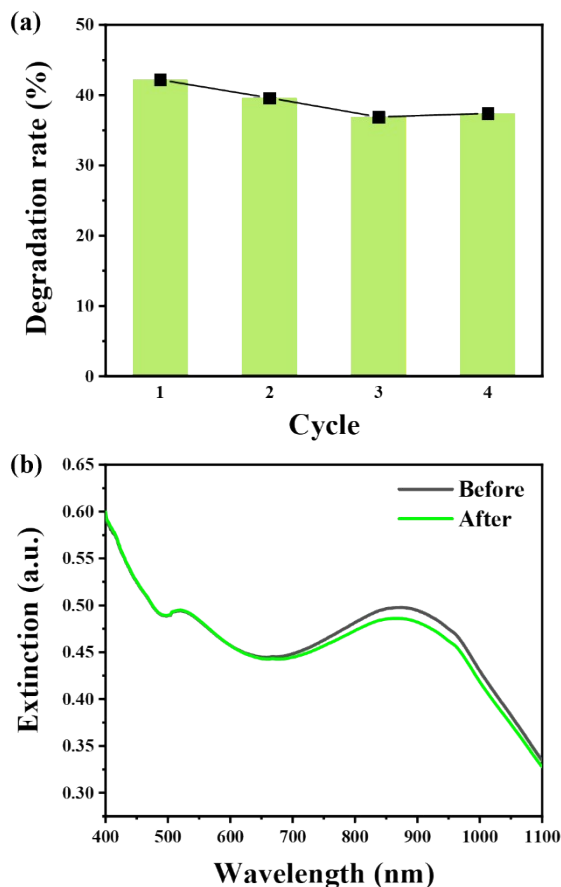


**Fig. S17** Stability of hollow dumbbell-like Au-PtCu NRs in a cycling test for the degradation of RhB. (a) Evolution of degradation rate in cycling test. (b) Extinction spectra of hollow dumbbell-like Au-PtCu NRs before and after photocatalytic process. After each degradation cycle, the catalyst was centrifuged and redispersed in RhB solution. The degradation rate remains high at 37.4% after four cycles. In addition, only a slight difference is observed in the extinction spectra before and after the degradation process.

## References:

- 1 S. Chavez, U. Aslam and S. Linic, *ACS Energy Lett.*, 2018, **3**, 1590-1596.
- 2 A. D. Rakić, A. B. Djurišić, J. M. Elazar and M. L. Majewski, *Appl. Opt.*, 1998, **37**, 5271-5283.
- 3 D. K. Roper, W. Ahn and M. Hoepfner, *J. Phys. Chem. C*, 2007, **111**, 3636-3641.